18th International Conference on Information Fusion
Washington, DC - July 6-9, 2015

Face Image Resolution Enhancement based on Weighted Fusion of Wavelet Decomposition

R. Raghavendra Christoph Busch
Norwegian Biometric Laboratory, Gjøvik University College, Norway
raghavendra.ramachandra@hig.no, christoph.busch@hig.no

***Abstract*—Automatic Border Control (ABC) systems based on face recognition are widely deployed in a border control scenarios. The efficiency of a ABC system depends on the early recognition of the capture subject as soon as he/she appears in the vicinity of the camera. However, due to various factors, including the change in illumination conditions, it is often challenging to capture a good quality face sample to facilitate the speedy biometric recognition with the ABC systems. In this paper, we propose a novel super resolution scheme to enhance the resolution of the captured face image. The proposed method is based on a weighted fusion of high frequency sub-band images obtained using Discrete Wavelet Transform (DWT) and Stationary Wavelet Transform (SWT). The weights are computed and assigned to the corresponding sub-band images of DWT and SWT by measuring both correlation and energy. Then, weighted sub-band images are fused using the sum rule. Finally, all these sub-bands are combined to generate a new resolution enhanced image using Inverse Discrete Wavelet Transform (IDWT). Extensive experiments are carried out using a semi-public ABC database that is comprised of 61 subjects. The database was captured in three different lighting conditions. Further, we also compare the performance of the proposed Super Resolution (SR) scheme with three well established state-of-the-art schemes. The experimental results have indicated that the proposed SR scheme can effectively improve the face recognition component of the ABC system even with low quality face samples.**

1. Introduction

The deployment of Automatic Border Control (ABC) gates that predominantly use face recognition to facilitate fast border control has gained a paramount interest. The operation of the ABC gates are governed by a protocol that basically allow the traveler (i.e. capture subject) to first present the passport, that will allow the ABC gate to read the biometric data (i.e. the face reference sample). Then, the traveler has to walk in a pre-assigned direction so that the probe face image is captured by the ABC system. Finally, the probe face image is compared with the reference face image stored in the passport to make a final decision on opening the gate for the user. With the deployment of more than 500 million ePassports, which store biometric reference samples, has boosted the applicability of the ABC system for highly reliable and accurate border control applications [1].

The ABC systems are normally installed in border control scenarios (e.g. Airports) that usually exhibits an uncontrolled scenarios. Furthermore the request for "On-the-Fly face recognition that refers to identifying a face of the subject as soon as he/she appears in the vicinity of the camera poses additional challenges that include fast response time as well as robustness to changes in face poses and illumination conditions. Thus most of previous work on improving the performance of the ABC is concentrated on assessing the quality of the captured probe face sample prior to making a final decision. The face quality estimation is well established with diverse algorithms that can be broadly classified into: into two groups [2]: (1) Face quality assessment based on reference image (2) Face quality assessment without reference image. The common face quality metrics includes in evaluating various measures like: Blur, Illumination, Pose, contrast and etc. These face quality metrics were summarized by the International Standardisation committee ISO/IEC JTC1 SC37 in ISO/IEC 29794-5 [3]. Most relevant are those quality metrics that can show a good prediction of the biometric performance according ISO/IEC 29794-5 [3], which can be validated by removing facial images that are labeled with poor quality scores in a technology test, which will reduce the recognition error. There are various methods available in the literature that includes empirical evaluation on five different quality measures such as contrast, brightness, focus, sharpness and Illumination for face quality measure [2], Local Binary Pattern (LBP) as a face quality metric [4], use of edge density, illumination and focus as a quality metrics [5], Greedy Pruned Ordering (GPO) algorithm [6]. In addition there also exist various quality measures that in particularly address face quality estimation from the video. Since the face video captures huge variation in pose, expression and illumination, it imposes lot of challenges, especially in terms of estimating pose [1]. The face quality estimation based on pose is introduced in [7], while patch based Discrete Cosine Transform (DCT) coefficients and a likelihood model based approach is presented in [8]. An extensive survey on existing face quality measures is presented in [9].

Even though face quality measures were predominantly studied in literature, there is still a limited experience in addressing the issue in operational ABC gates. A extensive evaluation of ABC gates was presented by Spreeuwers in [10] that also includes the study on different quality metrics to improve the accuracy of the face recognition subsystem. Despiegel et al. [11] provided a practical overview on estimating face quality in the context of ABC systems and illustrated the importance of a face quality measure for practical applications. Recently an empirical study in face quality measures using pose and texture based features for “On-the-Fly” face recognition from ABC gates are presented in [1].

Based on the above reported work we can conclude that by controlling the face quality with predictive quality metrics we can likely improve the face recognition performance of the ABC gate, but at the same time there is an operational risk that the ABC gate may exhibit a “timeout” if it fails to capture a face image with the expected sample quality. The “timeout” situation not only embarrassing for the capture subject but also plays a vital role in controlling procedures of the ABC gate especially in “On-the-Fly” face recognition scenarios. Thus, in this work, we explore the possible use of a single image based super resolution scheme to enhance the quality of the captured facial images to facilitate the early recognition of the traveler.

Most of the available super resolution schemes are designed to work with face video that requires certain video frames to be used in building a single super resolved image. A comprehensive survey on super resolution schemes is presented in [12] [13]. However, the use of multiple frames to construct a super resolved image will increase the response time of the ABC system to be used in practical scenarios. Thus, the use of single image based super resolution forms a crucial solution since it enhances the quality of each captured face image that will further improve the performance of the face recognition by allowing the gate to respond as soon as the face comparison score is greater than a predefined threshold. This motivates us to explore a single image based super resolution for reliable face recognition using ABC gates.

In this work, we propose a new scheme based on weighted fusion of stationary and discrete wavelet decomposition. Thus, given the captured face image from an ABC gate, the proposed method will first perform a multi-scale decomposition using both stationary and discrete wavelet transform to get the corresponding features. In the second step, we propose a novel scheme that can compute the weights by measuring energy from three sub-bands namely horizontal, vertical and diagonal obtained from both stationary and discrete wavelet transform. In the next step, we compute the energy of the sub-band images to be fused. We then measure the correlation between stationary and discrete sub band images to assign the weights before performing the fusion using the sum rule. Since the weights are computed by measuring the energy they will dynamically be adapted as needed. Extensive experiments are carried out on a dataset with 61 subjects. Image samples are captured by reflecting a real life scenario such that, the enrolment samples are captured in a studio setting using a 18.1 Mega pixel DSLR camera to comply with the photo capture guidelines that are defined by the International Civil Aviation Organization (ICAO) for electronic Passports. Then, probe samples are captured using a $MorphoWay^{\mathrm{TM}}$ [14] ABC system in a separate session. Note that the $MorphoWay^{\mathrm{TM}}$ [14] ABC system is used only for capturing the video of the subject and we have not used any proprietary software for recording, optimization, feature extraction and comparison.

The outline of the paper is as follows: Section 2 introduces the proposed single image based super resolution scheme, Section 3 presents the feature extraction and classification scheme used with ABC system, Section 4 presents the experimental protocols and Section 5 draws the conclusion.

2. Proposed Super Resolution Scheme

In this section, we present the proposed face super resolution based on the weighted fusion of discrete and stationary wavelet features. The proposed scheme is inspired on the work reported in [15]. We extend the work reported in [15] by introducing a novel weighted fusion such that weights are automatically computed for each face image captured using ABC system in both adaptive and dynamic manner. Figure 1 shows the block diagram of the proposed scheme that can be structured in three main steps namely: (1) Wavelet decomposition (2) Weighted fusion (3) Inverse Wavelet transform.

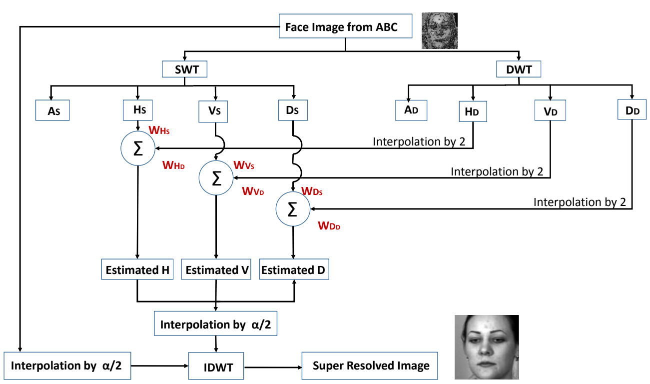

Figure 1: Block diagram of the proposed single image based super resolution scheme

2.1. Wavelet decomposition

Given the face image (probe) I_p captured using ABC system, we first perform the face detection and segmentation using using the Viola-Jones algorithm [16]. Since the ABC is in general installed in an indoor environment with constant back ground the use of the Viola-Jones algorithm appears to be the appealing choice by considering its robustness and performance in a real-time scenario. Even though the working distance of ABC is between 3 - 4 meters the use of the employed face detector has shown a good performance but it rarely results in false detection which can be addressed as mentioned in [17]. Let the detected and processed face image be termed as I_{pf}. In the next step, we perform the discrete and stationary wavelet transforms independently as follows:

$$[A_d, H_d, V_d, D_d] = DWT(I_{pf}) \tag{1}$$

Where, DWT indicates the Discrete Wavelet Transform (DWT) operation, A_d indicates the approximate sub-band, H_d indicates the horizontal sub-band, V_d indicates the vertical sub-band and D_d indicates the diagonal sub-band obtained using DWT. Before going to the next step, we interpolate three sub-bands (horizontal, vertical and diagonal) by a factor of 2 in order to match with the dimension of SWT features.

$$[A_s, H_s, V_s, D_s] = SWT(I_{pf}) \tag{2}$$

Where SWT indicates the Stationary Wavelet Transform (SWT) of the I_{pf}, A_s indicates the approximate sub-band, H_s indicates the horizontal sub-band, V_s indicates the vertical sub-band and D_s indicates the diagonal sub-band obtained using a stationary wavelet transform.

Figure 2 shows the qualitative results of the discrete and stationary wavelet decomposition. The use of stationary wavelet decomposition allows to address the translation variation and thus presents the better edge representation when compared with discrete wavelet transform. However, the use of stationary wavelet transform will result in redundant information as the output of each sub-band contains the same number of samples as the input image I_{pf}. Thus, a simple fusion of discrete and stationary wavelet features using sum rule as mentioned in [15] will not allow one to capture a complementary information useful for good quality super resolution image re-construction. This implies the need of intuitive way of capturing the useful information between discrete and stationary wavelet features by using weighted sum rule.

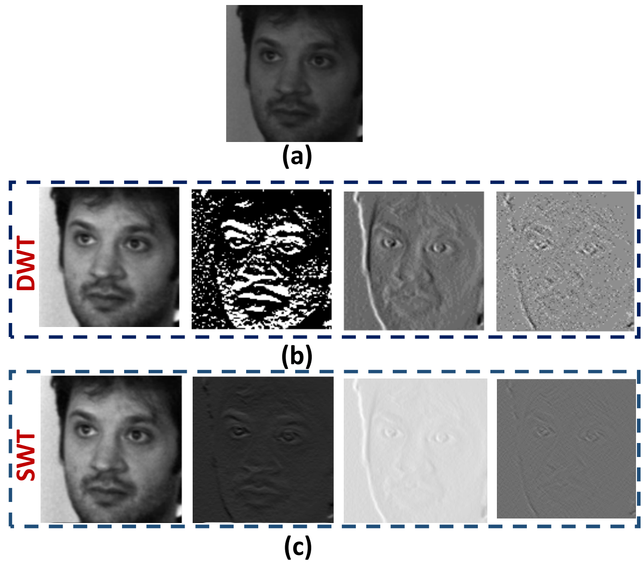

Figure 2: Illustration of different sub-bands obtained using discrete and stationary wavelet decomposition (a) face probe image (b) Discrete Wavelet Transform sub-bands (c) Stationary Wavelet Transform sub-bands

2.2. Weighted Fusion

The proposed weighting scheme can be structured in three main steps namely: (1) Energy computation (2) Correlation estimation and (3) Computing weights and fusion. The core idea of the proposed weighting scheme is to explore the independence between the discrete and stationary features so that more weight will be assigned to the features that has more energy to achieve super resolution reconstruction. The weights are computed individually on the horizontal, vertical and diagonal sub-band's which then fused using weighted sum rule.

2.2.1. Energy computation. Given the sub-band features from DWT features, we compute the energy for each of these sub-bands as follow:

$$ED_H = \sum_{x=1}^{R}\sum_{y=1}^{C}(H_d(x,y))^2 \tag{3}$$

$$ED_V = \sum_{x=1}^{R}\sum_{y=1}^{C}(V_d(x,y))^2 \tag{4}$$

$$ED_D = \sum_{x=1}^{R}\sum_{y=1}^{C}(D_d(x,y))^2 \tag{5}$$

Where, ED_H, ED_V and ED_D denotes the energy for horizontal, vertical and diagonal sub-band's computed using DWT.

Similarly, we also computed the energy on the sub-bands obtained using SWT as follows:

$$ES_H = \sum_{x=1}^{R}\sum_{y=1}^{C}(H_s(x,y))^2 \tag{6}$$

$$ES_V = \sum_{x=1}^{R}\sum_{y=1}^{C}(V_s(x,y))^2 \tag{7}$$

$$ES_D = \sum_{x=1}^{R}\sum_{y=1}^{C}(D_s(x,y))^2 \tag{8}$$

Where, ES_H, ES_V and ES_D denotes the energy for horizontal, vertical and diagonal sub-band's computed using SWT.

2.2.2. Correlation estimation. In the next step, we compute the correlation between each of these sub-bands from DWT and SWT to measure the complementary information. Thus, given the horizontal sub-band from DWT and SWT the Pearson Correlation Coefficient (PCC) can be calculated as follows: Let H_d be the reference image and H_s be the i^{th}

be the corresponding sub-band in the SWT, then the Pearson Correlation Coefficient (PCC) can be calculated as follows:

$$PCC_H = \frac{\sum (H_d - \hat{H}_d)(H_s - \hat{H}_s)}{\sqrt{\sum (H_d - \hat{H}_d)^2 \sum (H_s - \hat{H}_s)^2}} \quad (9)$$

Where, $\hat{H}_d$ represents the mean of H_d, $\hat{H}_s$ represents the mean of H_s and PCC_H denotes the correlation between horizontal sub-band images from DWT and SWT.

Similarly, we also compute the correlation measure corresponding to vertical and diagonal sub-bands to get PCC_v and PCC_d respectively.

2.2.3. Computing Weights. The proposed weight computation will use both correlation and energy computation. Given the correlation value for PCC_H corresponding to the horizontal band, we first compare the correlation value against a threshold value Th, which is determined empirically. Then weights are computed as follows:

$$W_1 = \begin{cases} \left[\frac{(Th - PCC_H)}{(1-Th)}\right] \times \frac{1}{2}, & \text{if } PCC_H < Th \\ 1, & \text{otherwise.} \end{cases} \quad (10)$$

$$W_2 = \begin{cases} 1 - W_1, & \text{if } PCC_H < Th \\ 0, & \text{otherwise.} \end{cases} \quad (11)$$

Such that $W_1 + W_2 = 1$.

Then in the next step, we assign the weights to each of these sub-bands by measuring the energy such that, the sub-band with highest energy will be assigned with highest weight as follows:

$$W_{Hs} = \begin{cases} W_1, & \text{if } ED_H > ES_H \&\& W_1 > W_2 \\ W_2, & \text{otherwise.} \end{cases} \quad (12)$$

and

$$W_{Hd} = 1 - W_{Hs} \quad (13)$$

Such that $W_{Hd} + W_{Hs} = 1$.

In this way, the proposed weighting scheme will try to capture the significant features by measuring both correlation and energy. Finally, the weighted fusion is carried out as follows:

$$Fu_H = (W_{Hs} \times H_s) + (W_{HD} \times H_D) \quad (14)$$

Where, Fu_H denotes the fused horizontal sub-band.

We repeat the above mentioned procedure on the remaining two different sub-bands namely vertical and diagonal to obtain a fused sub-image as Fu_V and Fu_D respectively.

2.3. Inverse Wavelet transform

Finally, we employ the Inverse Discrete Wavelet Transform (IDWT) to reconstruct the resolution enhanced face image. The IDWT is carried out on the fused sub-bands (Fu_H, Fu_V, Fu_D) and for the approximate band we use the normal image I_p which is interpolated by a factor of $\alpha/2$.

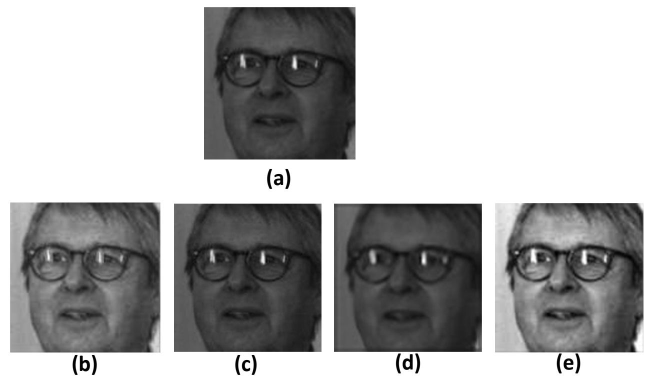

Figure 3: Qualitative results comparing the proposed method with existing state-of-the-art methods (a) Normal image (b) Super resolution using H. Demirel et al. [15] (c) Super resolution using J. Yang et al. [18] (d) Super resolution using T.Peleng et al. [19] (e) Proposed scheme

Figure 3 shows the qualitative results of the proposed super resolution scheme along with existing schemes [15] [18] and [19]. Figure 3 (a) shows the probe image captured from the ABC system under low lighting conditions. Figure 3 (b) shows the super resolution image obtained using H. Demirel et al. [15], Figure 3 (c) shows the super resolution image obtained using J. Yang et al. [18], Figure 3 (d) shows the super resolution image obtained using T. Peleng et al. [19] and Figure 3 (e) shows the super resolution image obtained using proposed scheme. Here it can be observed that, the proposed method results in an enhanced image with more sharpness and contrast when compared with other well-known super-resolution schemes.

3. Feature extraction and classification

In this work, we employ the feature extraction and classifications scheme based on the Log-Gabor (LG) transform as the feature extraction and Sparse Representation Classifier (SRC) as a classifier that can together constitute a comparison algorithm. This choice (LG-SRC) is made to achieve accurate and robust verification performance that was earlier used in [1] on ABC database and also by considering the fact that these techniques are popular and well established in the biometric community [20]. The LG filter employed in this work, has 4 scales and 8 orientations and we fix these values as the result of experimental trials and also in conformity with literature [20] [1]. It is very well demonstrated that the use of SRC will successfully tackle the presence of noise, illumination and occlusions. This motivates us to employ the

Figure 5: Examples of probe sample captured using camera 1 with three different lighting conditions

sparse representation for our present work. Here, we carry out l_1 - minimization via $SPGL_1$ solver based on spectral gradient projection [21] [1]. In this work, we obtain the comparison scores that directly correspond to the residual errors obtained using SRC [1].

4. Experiments and Results

This section present the experiments and results obtained using the proposed super resolution scheme and also we present the comprehensive comparison with three well established super resolution schemes. In this work, we employed the semi-public ABC face dataset collected using $MorphoWay^{\text{TM}}$ ABC system [1]. This database is comprised of 61 subjects that are captured by considering a real-life border control scenarios that requires to make the decision by comparing a high quality sample with the probe captured one. For each subject, there are 8 enrolled samples that are captured using high resolution Canon EOS 550D DSLR camera with various poses. While the probe samples are collected using $MorphoWay^{\text{TM}}$ ABC system under three different light conditions. The first lighting condition is simulated by setting the light intensity of 180 lux to reflect the dark overcast day, in the second condition, the light intensity is set to 450 lux that can reflect the light intensity during sunrise or sunset in the office building hallway, lastly the light intensity is set to 1500 lux that reflects the lighting condition of typical office hallway on a clear day.

Figure 4 shows the examples of the high quality enroled samples captures in studio setting. Figure 5 shows the example of the probe samples captured from camera 1 of the $MorphoWay^{\text{TM}}$ ABC system in three different lighting conditions. Figure 6 shows the examples of the probe samples captured from camera 2 of $MorphoWay^{\text{TM}}$ ABC system in three different lighting conditions.

4.1. Performance evaluation protocol

We followed the same experiment protocol described with the database [1]. Thus, the development subset is composed of only 3 subjects and the testing subset is composed of 58 subjects. We employed the development subset in order to determine the threshold value Th in our experiment which is then kept constant for all testing runs. However in this work we have used face probe samples corresponding

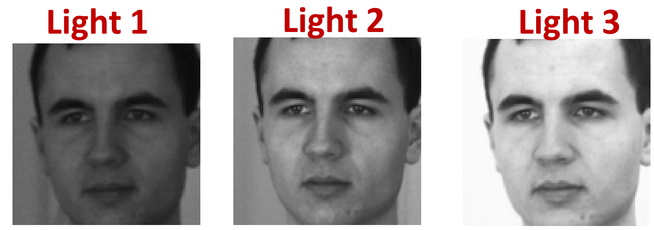

Figure 6: Examples of probe sample captured using camera 2 with three different lighting conditions

to camera 1 and camera 2 of the $MorphoWay^{\text{TM}}$ ABC system for simplicity.

4.2. Results and discussion

This section presents the results of the proposed super resolved scheme for the face ABC system. The results presented in this paper are reported in terms of Equal Error Rate (ERR), which is defined as a point, where the False Non Match Rate (FNMR) is equal to the False Match Rate (FMR). Thus the lower the values of EER, the better is the biometric performance. Further, we also present the ROC curves plotted as FMNR versus Genuine Match Rate (GMR) which is (GMR = 1-FNMR).

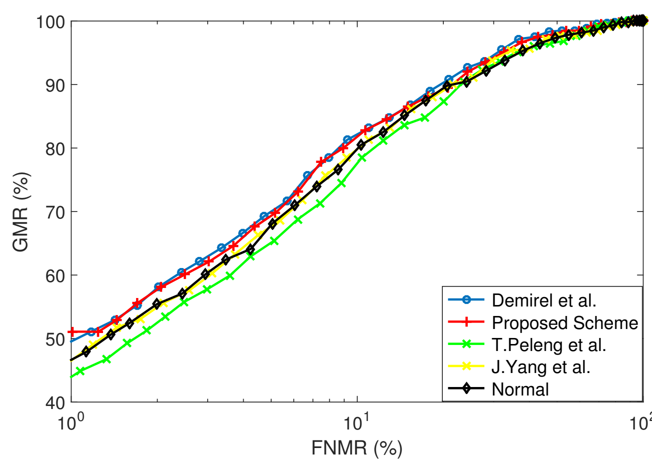

Figure 7: Verification performance of the proposed scheme on camera 1 Light 1

Figure 7, 8 and 9 shows the ROC curves that indicate the verification performance of the proposed scheme along with three well established super resolution schemes on the Camera 1 with lighting conditions 1, 2 and 3 respectively. Further, we also consider to include the performance of the ABC system without super resolution schemes that directly use the normal face probe image as captured by the camera. Based on the obtained results, it is interesting to observe that, the use of super resolution techniques will improve the overall performance of the ABC systems in all three lighting conditions. However, the application of the proposed scheme shows the best performance with an

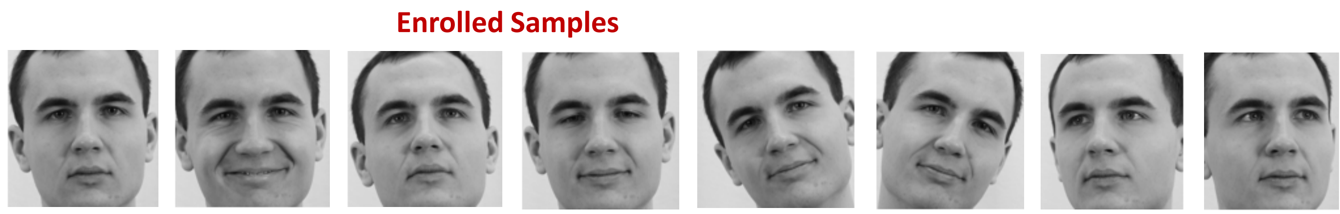

Figure 4: Examples of enrolled sample corresponding to one subject

TABLE 1: Qualitative performance of the proposed super resolution scheme

SR Algorithms	EER (%)					
	Camera 1			Camera 2		
	Light 1	Light 2	Light 3	Light 1	Light 2	Light 3
Without SR	14.74	12.64	11.16	16.16	14.69	12.46
Demirel et al. [15]	14.26	12.26	10.08	15.58	14.03	11.57
T. Pleng et al. [19]	14.02	13.91	10.05	16.19	14.49	11.98
J. Yang et al. [18]	14.40	12.44	11.19	14.67	14.32	12.33
Proposed Scheme	**12.86**	**11.46**	**9.78**	**14.56**	**13.06**	**10.57**

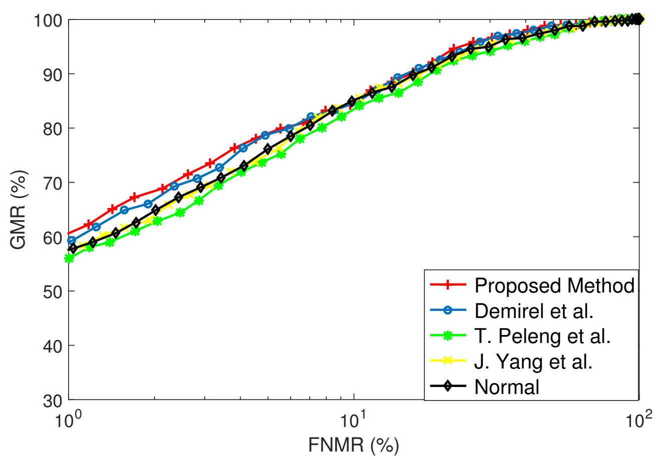

Figure 8: Verification performance of the proposed scheme on camera 1 Light 2

improvement of $GMR = 4.41\%$ @ $FMR = 10^0\%$ on lighting 1, $GMR = 4.47\%$ @ $FMR = 10^0\%$ on lighting 2 and $GMR = 5.82\%$ @ $FMR = 10^0\%$ on lighting 3 when compared with normal capture. This results dictates the applicability of the super resolution technique to improve the performance of the ABC system. Furthermore, it can also be observed that the proposed super resolution scheme outperformed the three different state-of-the-art schemes with the best performance of $GMR = 51.05\%$ @ $FMR = 10^0\%$ on lighting 1, $GMR = 62.14\%$ @ $FMR = 10^0\%$ on lighting 2 and $GMR = 66.82\%$ @ $FMR = 10^0\%$ on lighting 3. This further justifies the applicability of the proposed scheme.

Table 1 indicates the quantitative performance of the proposed scheme along with state-of-the-art super resolution schemes on ABC system. The results are presented for

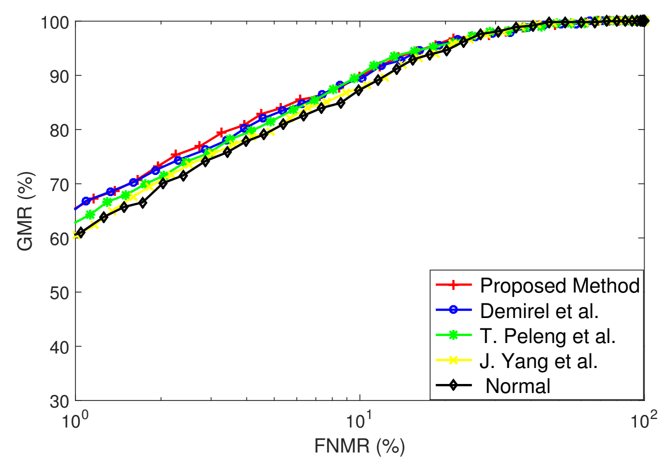

Figure 9: Verification performance of the proposed scheme on camera 1 Light 3

both camera 1 and camera 2 with three different lighting conditions. Here also it can be observed that, the proposed super resolution scheme outperforms the existing schemes with an $EER = 12.86\%$ on light 1, $EER = 11.46\%$ on light 2 $EER = 9.78\%$ on light 3 with camera 1. Similar observation can also be noted with camera 2, that again shows the best performance of the proposed scheme with $EER = 14.56\%$ on light 1, $EER = 13.06\%$ on light 2, $EER = 10.57\%$ on light 3. Thus, based on the obtained results, the proposed super resolution scheme shows the best performance when compared with state-of-the-art schemes and also indicates that the use of super resolution techniques will improve the performance of the ABC system.

5. Conclusion

This works introduces a novel super resolution scheme to improve the performance of the face ABC system. The proposed scheme is based on computing the wavelet coefficients using discrete and stationary wavelets whose subbands are fused by computing the weights that are adaptive and dynamic. The proposed weighting scheme is based on calculating the energy and correlation to capture a rich information from both discrete and stationary wavelet features. Extensive experiments are carried out on a semi-public ABC database with 61 subjects and indicate the best performance of the proposed scheme when compared with three well established state-of-the-art schemes. Furthermore, the results also indicate the superior performance of the ABC system with super resolved face images when compared with normal images. This further justifies the applicability of the proposed scheme for the practical applications.

Acknowledgments

This work is funded by the EU 7th Framework Program under grant agreement n^o 284862 for the large-scale integrated project FIDELITY. The authors also wish to express thanks to Morpho (Safran Group) for supporting this work by providing $MorphoWay^{\mathrm{TM}}$ prototype for this study.

References

[1] R. Raghavendra, K. B. Raja, B. Yang, and C. Busch, "Automatic face quality assessment from video using gray level co-occurrence matrix: An empirical study on automatic border control system," in *Proceedings of the 2014 22Nd International Conference on Pattern Recognition*, ser. ICPR '14, 2014, pp. 438–443.

[2] A. Abaza, M. A. Harrison, and T. Bourlai, "Quality metrics for practical face recognition," in *International Conference on Pattern Recognition (ICPR)*, 2012, pp. 3103–3107.

[3] ISO/IEC JTC1 SC37 Biometrics, *ISO/IEC TR 29794-5:2010 Information Technology - Biometric Sample Quality - Part 5: Face Image Data*, International Organization for Standardization, 2010.

[4] X. Gao, S. Z. Li, R. Liu, and P. Zhang, "Standardization of face image sample quality," in *Advances in Biometrics*, 2007, pp. 242–251.

[5] J. Beveridge, D. Bolme, B. Draper, G. Givens, Y. M. Lui, and P. Phillips, "Quantifying how lighting and focus affect face recognition performance," in *Computer Vision and Pattern Recognition Workshops (CVPRW), 2010 IEEE Computer Society Conference on*, 2010, pp. 74–81.

[6] P. J. Phillips, J. R. Beveridge, D. Bolme, B. A. Draper, G. H. Givens, Y. M. Lui, S. Cheng, M. N. Teli, and H. Zhang, "On the existence of face quality measures," in *IEEE International Conference on Biometrics: Theory, Applications and Systems, 2013*, 2013, pp. 1–6.

[7] K. Nasrollahi and T. B. Moeslund, "Face quality assessment system in video sequences," in *Biometrics and Identity Management*, 2008, pp. 10–18.

[8] Y. Wong, S. Chen, S. Mau, C. Sanderson, and B. C. Lovell, "Patch-based probabilistic image quality assessment for face selection and improved video-based face recognition," in *2011 IEEE Computer Society Conference on Computer Vision and Pattern Recognition Workshops (CVPRW)*, 2011, pp. 74–81.

[9] S. Bharadwaj, M. Vatsa, and R. Singh, "Biometric quality: a review of fingerprint, iris, and face," *EURASIP Journal on Image and Video Processing*, vol. 2014, no. 1, 2014.

[10] L. Spreeuwers, A. Hendrikse, and K. Gerritsen, "Evaluation of automatic face recognition for automatic border control on actual data recorded of travellers at schiphol airport," in *Biometrics Special Interest Group (BIOSIG), 2012 BIOSIG - Proceedings of the International Conference of the*, Sept 2012, pp. 1–6.

[11] V. Despiegel and S. Gentric, "Common mistakes on face recognition based on video," in *Proceedings of International Conference of the Biometrics Special Interest Group (BIOSIG)*, 2012, pp. 1–4.

[12] K. Nasrollahi and T. Moeslund, "Super-resolution: a comprehensive survey," *Machine Vision and Applications*, vol. 25, no. 6, pp. 1423–1468, 2014.

[13] E. Bilgazyev, S. Shah, and I. Kakadiaris, "Comparative evaluation of wavelet-based super-resolution from video for face recognition at a distance," in *Automatic Face Gesture Recognition and Workshops (FG 2011), 2011 IEEE International Conference on*, March 2011, pp. 559–565.

[14] "MorphoWay ABC," http://www.morpho.com/identification/border-control-242/controle-automatique/morphoway/?lang=en/.

[15] H. Demirel and G. Anbarjafari, "Image resolution enhancement by using discrete and stationary wavelet decomposition," *IEEE Transactions on Image Processing*, vol. 20, no. 5, pp. 1458–1460, May 2011.

[16] P. Viola and M. Jones, "Robust real-time face detection," *International Journal of Computer Vision*, vol. 57, pp. 137–154, 2004.

[17] R. Raghavendra, B. Yang, and C. Busch, "Accurate face detection in video based on likelihood assessment," *Norsk informasjonssikkerhetskonferanse (NISK)*, 2012.

[18] J. Yang, Z. Wang, Z. Lin, S. Cohen, and T. Huang, "Coupled dictionary training for image super-resolution," *Image Processing, IEEE Transactions on*, vol. 21, no. 8, pp. 3467–3478, 2012.

[19] T. Peleg and M. Elad, "A statistical prediction model based on sparse representations for single image super-resolution." *IEEE transactions on image processing*, vol. 23, no. 6, pp. 2569–2582, 2014.

[20] R. Raghavendra, B. Yang, and C. Busch, "Robust on-the-fly person identification using sparse representation," in *IEEE International Conference on Multimedia and Expo (ICME)*, 2013, pp. 1–4.

[21] J. Wright, A. Y. Yang, A. Ganesh, S. S. Sastry, and Y. Ma, "Robust face recognition via sparse representation," *IEEE Transactions on Pattern Analysis and Machine Intelligence*, vol. 31, no. 2, pp. 210 – 227, 2009.